Printable, Transparent and Flexible Touch Panels Working in Sunlight and Moist Environments

Tiina Vuorinen, Mari Zakrzewski, Satu Rajala, Donald Lupo, Jukka Vanhala, Karri Palovuori, Sampo Tuukkanen*

T. Vuorinen[1], M. Zakrzewski[1], Dr. S. Rajala[2], Prof. D. Lupo[1], Prof. J. Vanhala[1], Prof. K. Palovuori[1], Dr. S. Tuukkanen[1,§]
[1]Tampere University of Technology (TUT), Department of Electronics, Korkeakoulunkatu 3, P.O. Box 692, FI-33101 Tampere, Finland
[2]Tampere University of Technology (TUT), Department of Automation Science and Engineering, Korkeakoulunkatu 3, P.O. Box 692, FI-33101 Tampere, Finland.
E-mail: sampo.tuukkanen@tut.fi
[§]Present address: Aalto University, School of Chemical Technology, Department of Materials Science and Engineering, P.O. BOX 16200, 00076 Aalto, Espoo, Finland

Abstract
The ongoing revolution of touch-based user interfaces sets new requirements for touch panel technologies, including the need to operate in a wide range of environments. Such touch panels need to endure moisture and sunlight. Moreover, they often need to be curved shape or flexible. Thus, there is a need for new technologies suitable, for example, for home appliances used in the kitchen or the bathroom, automotive applications, and e-paper. In this work, the development of transparent and flexible touch panels for moist environments is reported. A piezoelectric polymer, poly(vinylidene difluoride) (PVDF), is used as a functional substrate material. Transparent electrodes are fabricated on both sides of a PVDF film using a graphene-based ink and spray coating. The excellent performance of the touch panels is demonstrated in moist and underwater conditions. Also, the transparent device showed very small pyroelectric response to radiative heating in comparison to a non-transparent device. Solution processable electrode materials in combination with functional substrates allow the low-cost and high-throughput manufacturing of touch panels using printing technologies.

1. Introduction
During recent years the user interfaces of electronic devices have undergone a revolution, changing from old-fashioned button-type controls towards embedded touch panels and touch screens. It is expected that transparent control panels will spread from mobile devices to be embedded as a part of built environment. This raises major challenges to touch panel technology with requirements like functionality in moist or underwater environment, integration into curved surfaces, flexibility, temperature stability, and mechanical durability.

Printing and other solution processing technologies have raised interest in the electronic industry, and the push towards organic and printed electronic systems is strong at the moment.[1] The most interesting perspective of the printing is enabling of high throughput manufacturing of electronic devices. Furthermore, the use of solution processable organic and molecular materials in the fabrication of electronic devices is becoming popular due to their potential ecological benefits, such as recyclability or decomposability.[2] Even if organic electronics cannot at present compete in performance with silicon technology, it has great potential to be utilized in large-area applications and disposable low-end products.[1] Using small molecules, polymers, or carbon based nanomaterials, instead of metals and solid-state semiconductors, gives rise to transparent electronic circuits, which is a prerequisite for touch panel technology.

The use of conducting polymers, such as poly(3, 4-ethylenedioxythiophene):poly(styrenesulfonate) (PEDOT:PSS), or carbon based nanomaterials, such as graphene and carbon nanotubes (CNT), enable fabrication of flexible or stretchable electrodes for sensor applications.[3-5] These materials also have their limitations. Although a single CNT can carry a few mA current,[6] contact resistances between crossing tubes limit the overall conductivity of a randomly oriented CNT network.[7] Nevertheless, highly conducting CNT networks have been recently demonstrated in supercapacitors,[8–12] which are promising future energy storage devices. While the degradation of conductivity of PEDOT:PSS under ambient conditions has conventionally been a challenge,[13] highly stable formulations have been recently obtained.[14]

Nowadays, there are several competing touch panel technologies available, but they all have some limitations such as diminished functionality in moist and wet environment. Water-proof touch panels are however required for example in outdoor interactive panels and automotive touch panels as well as control panels in swimming pools or shower walls and mirrors. Capacitive, resistive, and optical sensing are the three major technologies used in multi-touch sensing applications.[15] The drawback with optical sensing methods is that they all are highly affected by the surrounding lighting and cannot be used with bended surfaces. A resistive touch panel consists of two conductive sheets (coated for example with indium-tin-oxide) and a layer of dot spacers in between. Pressing the panel causes the conductive top sheet to physically yield and contact the bottom layer.[18-20] The dot spacers prevent the contact of the top and the bottom sheets when the panel is not pressed. Thus, water droplets or sunlight do not cause artefacts in resistive panels. However, when immersed in water, the hydrostatic pressure yields the top sheet similarly as touch. With high enough hydrostatic pressure, this saturates the panel. For example, the hydrostatic pressure in 1 m depth corresponds to a medium touch pressure (1 N cm^{-2}). Hence, resistive touch panels face a trade-off between the sensitivity and underwater functionality. Capacitive sensing can be divided into two methods: surface capacitive and projected capacitive sensing. In projected capacitive touch sensing, the capacitance at each addressable electrode is measured.[21] A finger or a stylus close by disturbs the electromagnetic field and alters the capacitance.

A touch on the surface can be measured from a change in the capacitance.[22-25] The major disadvantage of capacitive touch technology is the disturbance in moist environments. Normally, neither surface nor projected capacitive method is capable of functioning under water or with liquid droplets on the panel. Recently, examples of underwater projected capacitive sensing have been presented, however, with the expense of increased false touch rate.[26, 27] Further drawbacks are the lack of pressure sensitivity, poor touch time resolution to the exact touch moment and dependence on the dielectric properties of the touching instrument. In practical applications, this means false detection with fast touch typing if the user is resting fingers on keys without intention to press the key and inability to detect fingers with gloves on.

One promising technology for touch devices is piezoelectric sensing.[28] The advantage of piezoelectric polymer films, such as poly(vinylidene difluoride) (PVDF), is that they are thin, flexible, lightweight, and they can be integrated into various shaped surfaces such as pillars or cylinders. The PVDF film can be easily sealed hermetically and thus, it can be used in several sensing applications due to its versatile properties. For instance, PVDF has a wide frequency range (from 0.001 Hz to 10^8 Hz) and a vast dynamic range (from 10^{-8} to 10^6 psi).[42] In addition, the PVDF material is sensitive to pressure changes, not to a static pressure. For example, hydrostatic pressure does not saturate a piezoelectric touch panel. A touch panel technology based on printable piezoelectric sensors has recently been demonstrated.[29–31] However, flexible, transparent, and water-proof piezoelectric touch panels have not been reported to date. Piezoelectric polymer films are interesting also for physiological measurements[3,4,32,33] and energy harvesting application.[34–38] In addition, piezoelectric polymer films have previously been used to manufacture flexible and transparent loudspeakers.[39, 40]

This paper reports the successful implementation of a transparent and flexible piezoelectric touch panel technology. Unlike most competing technologies, these touch panels can also be utilized in moist environments due to the sensitivity to applied force instead of the capacitance change. In this paper, we demonstrate underwater functionality for the first time. In addition to the advantages of piezoelectric sensing over the existing technologies, the use of a piezoelectric polymer film as a functional substrate material enables high
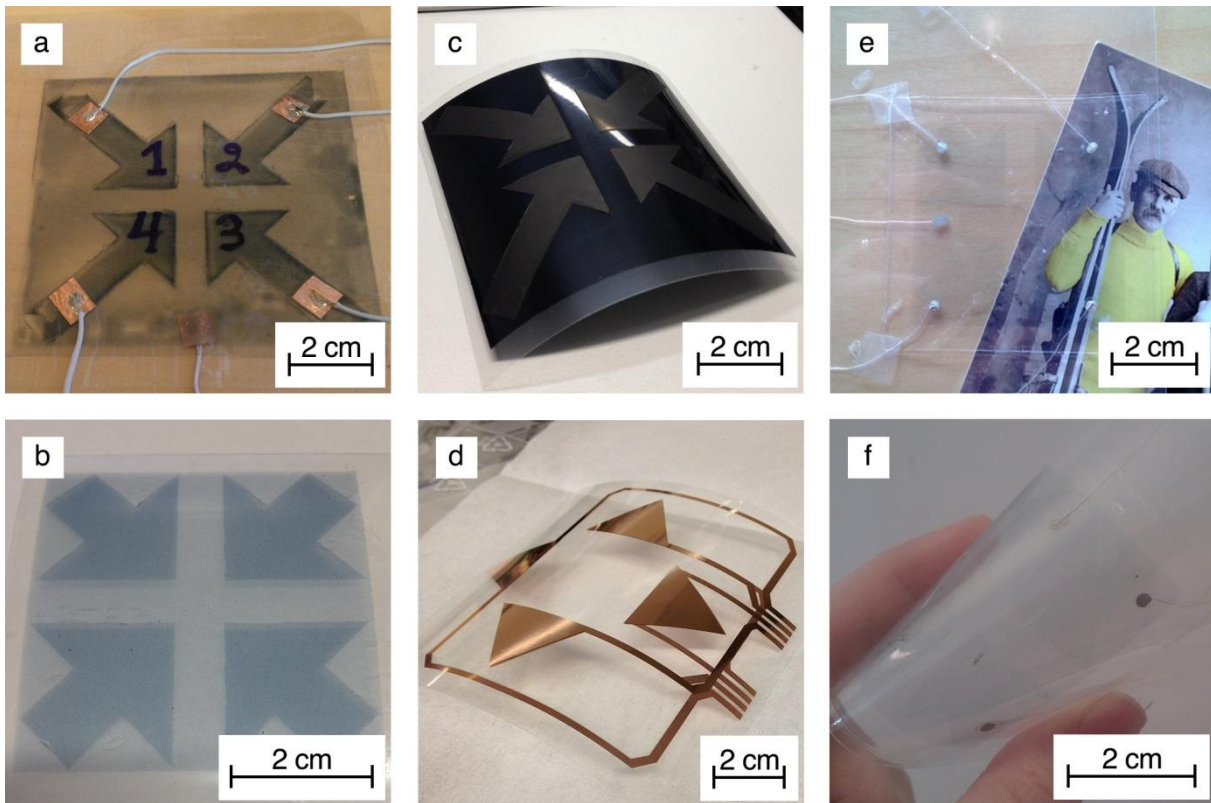
Figure 1. Photos of the samples (a) S1, (b) S2, (c) S3, (d) S4 and (e-f) S5. The high transparency (e) and bendability (f) of the sample S5 is illustrated as placed above a postcard and when bent.

throughput manufacturing using roll-to-roll printing techniques. Transparent electrodes are made here from a graphene-based ink, which gives sufficient conductivity for this type of application.

2. Results and Discussion
2.1. Samples and electrode properties

The electrodes for piezoelectric film-based touch panels were fabricated from three different nanostructural carbon inks. One of the inks contained a CNT/xylan nanocomposite, and the two others were composites of graphene and a conducting polymer. Electron-beam evaporated copper electrodes were used as reference samples. Photos of fabricated samples are shown in **Figure 1**. The electrode deposition was done on both sides of the PVDF film to accomplish the triple-layered structure, in which four arrow-shaped keys formed the top layer on the PVDF, and one large square pattern formed a ground plane on the opposite side of the film (see Figure 1(a-c)). Two different solution-processing methods, doctor blading and spray-coating, were used for electrode deposition, and the patterning was done using mechanical masks. The CNT and the graphene screen inks were spread with a doctor blade across the mechanical mask, and the graphene inkjet ink was spray-coated with an airbrush (Silverline). For the reference sample 100

nm thick copper electrodes were fabricated on PVDF film using vacuum evaporation and a mechanical mask.

The measured sheet resistances for different electrode materials are listed in **Table 1**. The mean and the standard deviation from 25 repetitive measurements per each sample are presented i.e. the measurement was repeated five times for each key and the large ground plane.

The piezoelectric touch panels were laminated with a pouch-laminator (Fellowes, Inc.) to provide a waterproof enclosure and some mechanical support. To ensure the waterproof enclosure during water immersion tests, a water absorption test was executed according to the European standard EN ISO 62:2008[41] to measure how much the lamination covering the panels would absorb water in 24 h. The water absorbance measurements showed only a 0.37 wt-% change in average, which indicates that the lamination material was suitable for water immersion tests.

The transparency and the flexibility of the thin graphene sample S5 are seen in Figure 1e and 1f. The photonic transmission was measured in the 420-650 nm range following the standard MIL-DTL-62420. The transparency of the arrow-shaped keys in the sample S5 was 64.7 %. The transparency can be considered good because the transparency of the
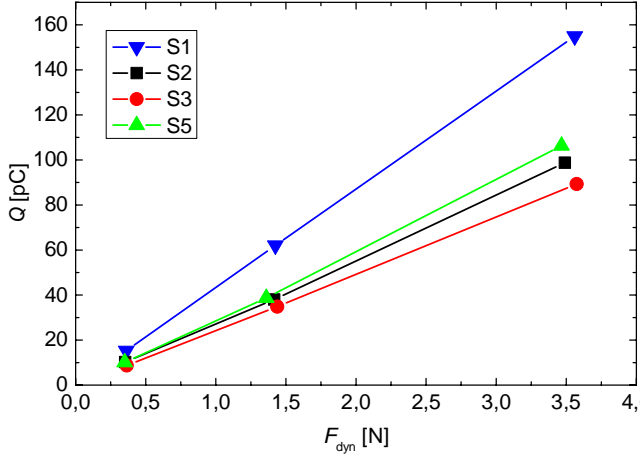
Figure 2. Linearity of the touch sensors S1, S2, S3 and S5. The charge developed by the sensor [pC] is presented as a function of the dynamic excitation force [N] applied to the sensor.

sole lamination film was 74.1 % and the transparency of the lamination film and the PVDF substrate together was 69.6 %. Thus, most of the optical losses are resulting from the interference and reflections in the lamination films.

Table 1. The measured sheet resistances and sensitivities.

Sample name	Electrode material	Sheet resistance [Ω sq^{-1}]	Sensor sensitivity [pC N^{-1}]
S1	Graphene screen ink	620 ± 10	44.6 ± 4.1
S2	Graphene inkjet ink, thick	76 ± 8	29.7 ± 5.2
S3	CNT/xylan ink	68 ± 8	26.4 ± 2.9
S4	Copper	1.0 ± 0.2	-
S5	Graphene inkjet ink, thin	1400 ± 20	34.9 ± 5.8

2.2 Sensor sensitivity measurements

Table 1 summarizes the measured sensor sensitivities for each sensor with solution-processed electrodes (S1-S3, S5). The sensor sensitivity is presented as the mean ± standard deviation of eight repetitive measurements per each sensor type. Only one key of each sensor type is measured. As presented in Table 1, the electrode material affects the sensitivity. On the other hand, also the lamination may affect by producing additional stresses to the PVDF material.
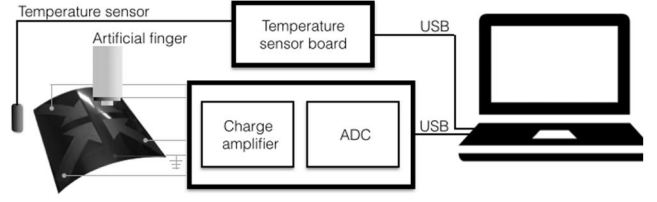

Figure 3. The sensor response measurement setup.

The touch sensor sensitivities were also measured using three different forces (approximately 0.3 N, 1.3 N and 3.4 N) to find out their dependence on the touch force. The forces correspond to low, medium and high forces used with touch panels (evaluated with a balance). The results are shown in **Figure 2**. It was found that the amount of generated charged increased very linearly as a function of applied force. Hence, the sensitivities of the sensors are constant for various force regimes. Based on the sensitivity measurements, repeatability was good and fatigue effect was not observed.

2.3. Panel operation in dry and moist environments

The response of the touch panels were measured using the setup described in **Figure 3** consisting of a charge amplifier, and an analog-to-digital converter (ADC). The temperature of the touch panel was measured simultaneously.

In addition to pressing the panel with a finger, a custom-made stylus was used in water immersion tests to rule out the pyroelectric phenomena caused by a human finger maintaining the body temperature. The stylus consisted of a metallic weight formed into a cylinder with a rubber tip on top of the cylinder mimicking a real fingertip.

To demonstrate that the panel works in a moist environment and underwater, several tests were conducted in different measurement configurations both in a laboratory environment and by immersing them in a sink filled with water. **Figure 4** shows the response signals obtained in the shower, in dry ambient air, and in underwater conditions. It can be noticed from Figure 4 that there is no cross-talk effect between two adjacent keys. However, when the panels were not fixed to the rigid surface during the operation, considerable cross-talk between adjacent keys was observed because of the bending of the PVDF film.
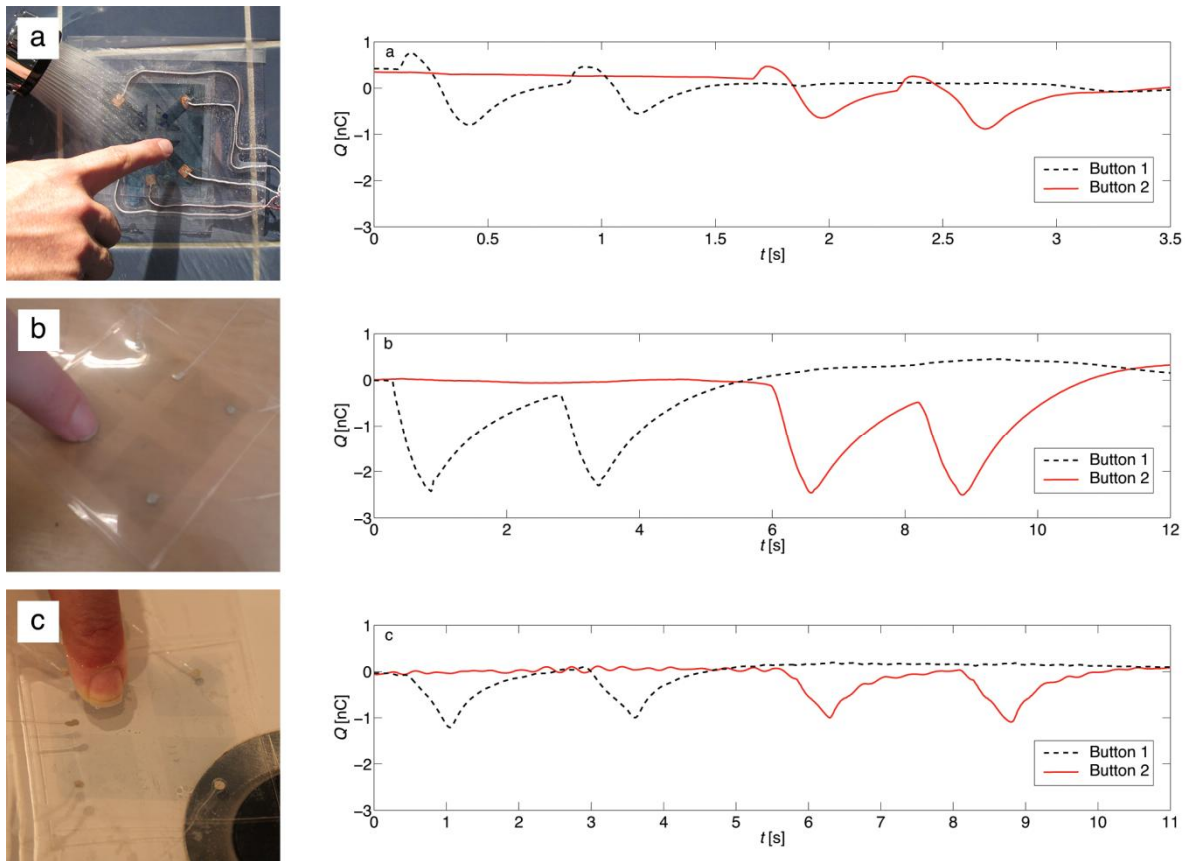
4

Figure 4. The response from (a) the shower tests with sample S1 and from (b-c) the immersion tests before and during the immersion with sample S5.

2.4. Pyroelectric and piezoelectric responses

There are two simultaneous effects, pyroelectric and piezoelectric, which define the overall touch response of piezoelectric panels.[31] When a key is pressed, the two responses are superimposed in the resulting signal: mechanical pressing causes a piezoelectric effect, and temperature change causes a pyroelectric effect. These effects happen simultaneously, making them hard to separate. The pyroelectric response signal is proportional to the temperature difference between the finger/stylus and the touch panel, whereas the piezoelectric response is proportional to the applied force. Typically the pyroelectric effect takes place at lower frequencies than the piezoelectric effect due to the slow heat transfer mechanisms.[42] However, when the PVDF material has stabilized to a certain temperature, the material properties remain constant over time. The phenomena of simultaneous piezo- and pyroelectric effects are demonstrated in **Figure** 5, where the response curves from sample S5 immersed in 20 °C and at 50 °C water are plotted in the cases of pressing with finger and stylus. When the temperature of the finger/stylus was higher than the temperature of the touch panel, the measured change is negative (see Figure 5a-b); and when the

temperature of the touch panel exceeded the temperature of the finger/stylus, the observed signal direction is positive (see Figure 5c-d). Each graph in Figure 5a-d presents the response signals from two adjacent keys and each key is pressed twice either with a finger or stylus.

2.5. The operation in sunlight

In real life applications, when the touch panel is exposed to the sunlight, the absorption of heat results to a pyroelectric response signal. The touch panels were tested during a sunlight exposure, and the resulting signal responses are shown in **Figure 6a** for samples S3 (CNT/xylan) and S5 (Graphene, thin). To compare the pyroelectric and piezoelectric responses, the magnitude of the response of pressing keys with a stylus is shown in Figure 6b with an equal scale. In Figure 6a, a large pyroelectric response is seen in the sample S3. In fact, the response is so large that it saturates the ADC. This is solely a pyroelectric effect as no touch or pressure change was involved. The response in graphene (S5), on the other hand, is on the same order of magnitude as the pressure response. However, the pyroelectric effect is much slower and thus it may be possible to separate the effects based on response speed. The
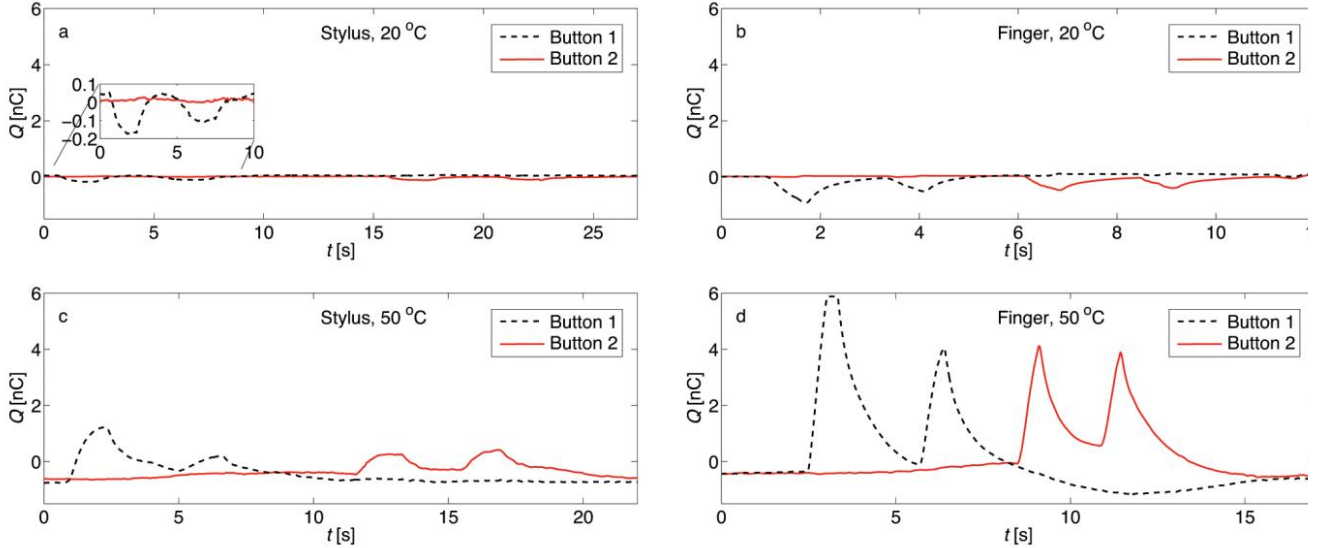
Figure 5. Positive and negative pyroelectric response curves from sample S5 obtained at two temperatures, (a-b) at 20 °C and (c-d) 50 °C, and touching either with (a, c) stylus and (b, d) finger. Each key is pressed twice.

result is expected: the more transparent the panel is, the less it will be warmed in the sunlight, and the smaller pyroelectric response is seen in the signal. The insensitivity to sunlight is a highly desirable effect in touch panels, especially in outdoor applications.

In comparison, Rendl et al. proposed the use of an additional foil which acts as a temperature absorbing layer to reduce the pyroelectric response.[31] However, such absorbing layer plate is not transparent, which is the key characteristic of our proposed touch panel technology. Furthermore, the absorbing layer decreases the effect only about 60 % which is not enough in practical applications.

2.6. The temperature dependency of the response
The charge generated by the sensor versus temperature graphs obtained from the water immersion experiment are presented in **Figure 7**. The first and last data points at 30 °C room air (marked with 'x') are measured before and after the immersion, respectively. The solid square markers represent keystrokes done underwater with the stylus, and the open sphere markers represent the keystrokes done with a finger. As observed from the curves, the response signals are linearly dependent on the water temperature.

A highly temperature-dependent response was observed in the case of finger touch because of the larger role of pyroelectric effect. However, in the case of stylus touch, the temperature-dependency is less significant. It is important to notice from Figure 7 that a stylus touch does not heat (or cool) the panel

electrode as much as a finger touch. This indicates that the piezoelectric effect plays a bigger role when the panel is not heated (or cooled) by the finger. In all cases, the response to touch was largest when the water temperature was furthest away from the stylus/ finger temperature.

3. Conclusion
In this paper, it has been demonstrated how flexible and transparent touch panel electrodes can be manufactured from a solution processable graphene-based ink, using a spray coating method, onto a PVDF film. Other solution processable electrode materials and e-beam evaporated copper electrodes were used for comparison. Transparent and flexible panels can be integrated e.g. on curved, rigid surfaces and thus, they offer more possibilities for design issues. The results showed that touch panels were functional both in moist environment and underwater. In the water immersion tests, the overall response of the touch panel was the summed response from the piezo- and pyroelectric effects. It was observed that a finger touch response showed a higher temperature-dependence than a stylus touch response, because of the larger role of pyroelectric effect. In the sun exposure test, the sunlight had a much smaller impact on the transparent graphene-based electrodes than on the black CNT-based electrodes. These results show that piezoelectric PVDF touch panels with graphene-based solution processed electrodes are convenient, for example, for outdoor applications, because water and sunlight would not disrupt their functionality.
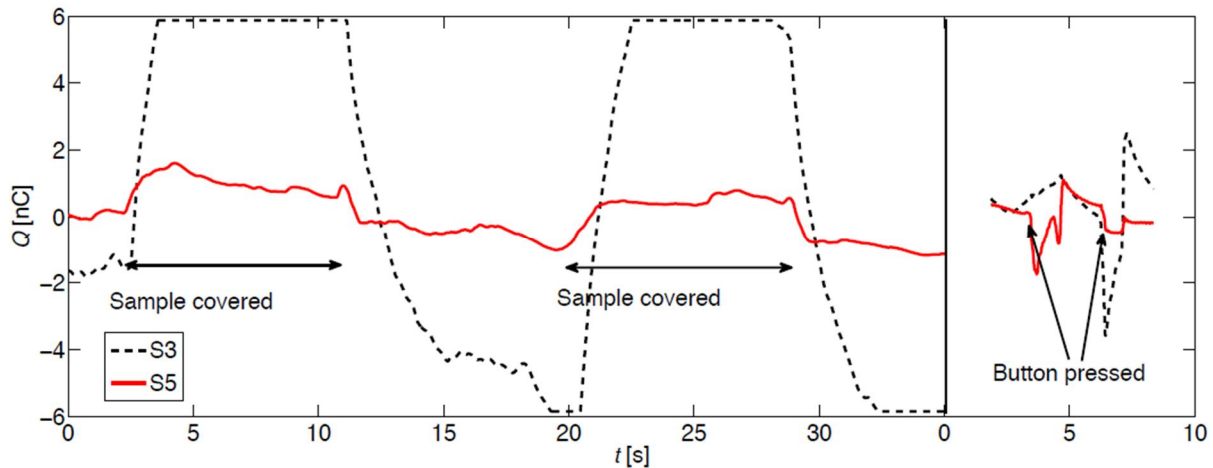
Figure 6. Sunlight exposure test results from the samples S3 and S5. (a) The response signal in sunlight vs. in the dark (sample covered). (b) The response while pressed with the stylus in sunlight. The transparent graphene sample S5 shows much smaller pyroelectric response (less radiative heating) than the non-transparent CNT sample S3, whereas the magnitude of the pressure response is on the same order of magnitude in both samples. Also, the effect of the pressure response is much faster than that of the light exposure. Note that the scale is the same in both the figures.

4. Experimental Section

Materials: A CNT/xylan nanocomposite ink, which was still in development phase, was obtained from Morphona Ltd.[9,10] and graphene/conductive polymer composite inks were purchased from Innophene. Graphene inks were PHENE+ I3015 formulated for inkjet printing, and PHENE+ P3014 formulated for screen printing. The CNT ink has a 3.5 wt% solid content that includes 2.5 wt% of CNT and 1 wt% of xylan. The Innophene inkjet ink consists of 1–5 wt% polymer and 1–5 wt% graphene and it also includes organic solvents such as diethylene glycol and ethanol. The ingredients of the Innophene screen printing ink were 1.0–5.0 wt% polymer, less than 1.0 wt% graphene, and solvents such as diethylene glycol, ethanol, and propylene glycol. A silver flake ink[3] and a copper adhesive tape were used to attach wires to the panel. The silver flake ink (Acheson Electrodag from Henkel) had solid content of 72 wt% containing n-propylacetate as the solvent.

A piezoelectric 110-µm-thick PVDF film (purchased from Measurement Specialities Inc.) was used as the functional substrate material for all the fabricated touch panels. PVDF is a semicrystalline polymer having a solid and homogenous structure. The change in film thickness due to an external force compressing the film generates a charge and thus, a voltage to appear at the electrodes. This phenomenon is known as the direct piezoelectric effect. The PVDF material is not suitable for static measurements and only the change of an external

pressure can be measured. The piezoelectric coefficients provided by the manufacturer are $d_{33} = -33 \cdot 10^{-12}$ C N^{-1} (compression) and $d_{31} = 23 \cdot 10^{-12}$ C N^{-1} (stretching).[42] The piezoelectric coefficients of the PVDF material tend to increase with temperature; the temperature dependence is reported e.g. in references[42, 43]. The PVDF material is also pyroelectric: as the film is heated, the dipoles within the film exhibit random motion by thermal agitation, causing a reduction in the average polarization of the film and thus generating a charge build up on the film surfaces. The amount of electrical charge produced per degree of temperature increase is described by the pyroelectric charge coefficient ($p = 30 \cdot 10^{-6}$ C m^{-2} K^{-1}).[42]

Manufacturing methods: A laser cut stencil (purchased from Easy-Cad Oy) was used as a mechanical mask for copper evaporation. Masks used to define ink patterns were fabricated from 125-µm-thick poly(ethylene terephthalate) (PET) film (Melinex ST506 from Dupont), and cut-out holes were made by carving them with a craft knife. The arrow shaped keys were chosen to simulate a remote control device for tuning of volume and channel in a media player. Temporary bonding adhesive (Zig 2-Way Glue) was used to secure PET masks in place during coating. The adhesive also prevented the ink from leaking underneath the mask. During the spray-coating, the sample was placed on top of a 60 °C hot plate so that the hot plate would dry the ink just enough to ensure even layer formation. Without the hot plate, the ink aerosol
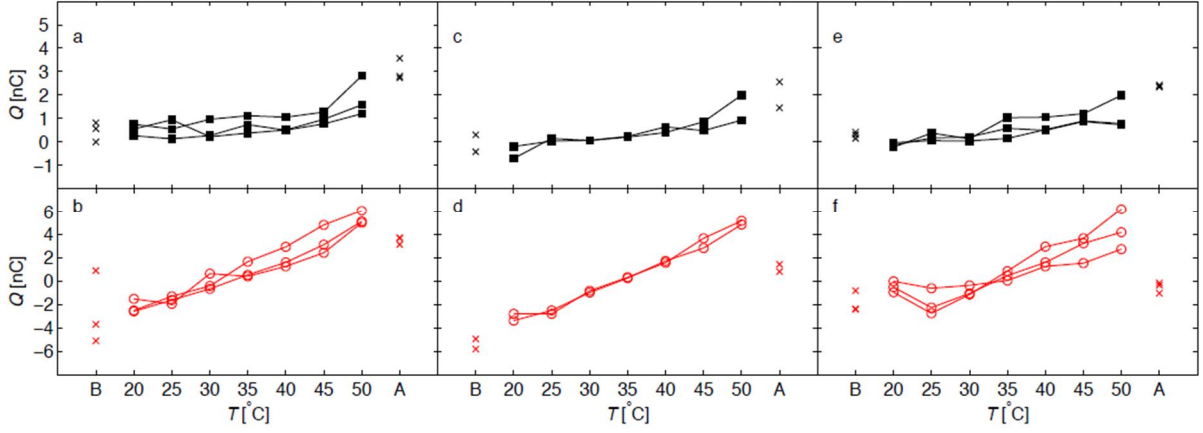
Figure 7. Measured response amplitudes in underwater conditions for samples (a-b) S2, (c-d) S4 and (e-f) S5 when pressing sequence is done by the stylus (black squares) and by the finger (red circles). A-axis tick labels B and A stands for 'before' and 'after' the immersion test, respectively.

would agglomerate and form large individual drops on the surface of the PVDF. After each electrode deposition, samples S2 and S5 (Graphene, inkjet) were dried in a convection oven; the thicker panel for 15 min at 65 °C and the thinner panel for 8 min at 65 °C. Since the electrodes were deposited on both sides of the PVDF substrate, each panel underwent two oven treatments. After the ink deposition, the manually doctor-bladed sample S3 (CNT) was left to dry at room temperature and sample S1 (Graphene, screen) was dried in a convection oven for 10 min at 60 °C. The wiring for the piezoelectric touch panels was made by attaching a wire with silver ink to each of the keys and one to the square pattern. In the thicker graphene panel, insulated single-strand wires were used. However, in the thinner graphene panel, individual wire strands from an insulated wire bundle were used to maximize the transparency of the touch panel.

Sheet resistance measurement: A multimeter (Keithley 3435 100 W SourceMeter) and an in-house four-point probe were used in sheet resistance measurements.[3] The four-point probe has four spring probes, two current-carrying and two voltage-sensing, placed in line with equal spacing ($s = 3$ mm). Finally, the corrected sheet resistance was calculated using equation $R_S = G \times (\pi/\ln2) \times (V/I)$, where I is the applied current between the two outermost probes, V the measured voltage between two innermost probes and G an additional geometric correction factor which is determined by sample dimensions and the probe spacing.[44] The geometric factors for arrow patterns were $G = 0.635$.

Water absorption measurement: The procedure for determining the water absorption was done by cutting six 6.1 cm x 6.1 cm pieces out of a single, previously heat laminated, lamination pouch (composed of two 125 μm thick sheets). Samples were dried in a convection oven at 50 °C for 24 h, and after cooling back to room temperature, they were immersed in distilled water for 24 h. To determine the percentage change on mass, indicating to the amount of water absorbed, each sample was weighed before and after the water immersion.[41]

Optical transparency measurement: The transparency measurement was conducted based on the principles of the standard MIL-DTL-62420. The photonic transmission at wavelength range 420–650 nm was measured using an Ocean Optics spectrometer. The incident light is produced by halogen lamp D65. The light is transferred to the sample through an optical fibre and collected again by a second fibre transferring the light to the photodetector.

Sensitivity measurements: The sensor sensitivity measurement setup is previously reported.[3], [32]. Briefly, the Brüel & Kjaer Mini-Shaker Type 4810 was used in the sensitivity measurements to provide a dynamic excitation force. A sinusoidal input for the shaker was provided with a Tektronix AFG3101 function generator. A pretension, which produces static force of about 3 N, was used to keep the sensor in place. A commercial high sensitivity dynamic force sensor (PCB Piezotronics, model number 209C02) and a load cell (Measurement Specialties Inc., model number ELFS-T3E-20L) were used as reference sensors for the dynamic excitation and static forces. The charge developed

by the sensor was measured with a custom-made combination of a charge amplifier and a 16-bit AD-converter.

The sensor key element was excited a 10 seconds period with a dynamic, sinusoidal 2 Hz input signal of 1000 mV (peak to peak), resulting in approximate force of 1.3 N. The four excitations were done by applying the force in the middle of the sensor. The excitations were repeated on both sides of the sensor, resulting in a total of eight excitations per sensor key element.

Sensor response measurement setup: Sensor signals need to be amplified before digitizing. A charge amplifier with the amplification of 0.210 V $(nC)^{-1}$ was used. The conversion was done with a 16-bits analog-to-digital converter (ADC) (model ADS8344 from Texas Instruments). A sampling frequency of 57 Hz was used. With this set up, we were able to measure charges between -6 nC and 6 nC. The water temperature was measured simultaneously during the response measurement with a temperature sensor (model 18B20 from Dallas), which was attached to the glass plate next to the samples with a double-sided adhesive tape. A schematic of the sensor response measurement setup is shown in Figure 3.

Sunlight exposure test: For the sunlight exposure test, the thin graphene sample S5 and the CNT sample S3 were attached side-by-side to the same transparent plastic plate with double-sided tape. This ensured that environmental changes happened simultaneously to both samples. The plate was positioned next to an open door and turned towards the sun. The ambient air temperature was 19 °C in the beginning of the measurement. Then, a metal plate was positioned to block the sun exposure to the samples.

Moist environment tests: In the shower tests, the sample S1 was attached to the wall using PET film and temporary bonding adhesive. Tests were performed under a spray of water in a shower. The functionality tests for samples S2-S5 were performed in both laboratory environment and by immersing them in a sink filled with tap water. The samples were immersed in the depth of approximately 3.5 cm in stationary water. The sequence of pressing test consisted of two keystrokes per key with both a finger and a stylus. From the response curves, a maximum deviation (either positive or negative) from the signal base level is interpreted as a response value.

In the water immersion tests the first test sequence was performed on a table before the immersion. The next six sequences were performed underwater, and between each sequence, the water temperature was increased by 5 °C, starting from a temperature of 20 °C to the maximum temperature of 50 °C. After the immersion, the touch panel was lifted out from the sink, and the pressing sequence was executed for the last time after the panel had cooled down to approximately 30 °C.

[1] White Paper "*OE-A Roadmap for Organic and Printed Electronics*", 5th edition, Organic and Printed Electronics Association, Frankfurt, **2013.**

[2] *Towards Green Electronics in Europe,* Strategic Research Agenda (SRA) for Organic and Large-Area Electronics (OLAE), **2009**.

[3] S. Tuukkanen, T. Julin, V. Rantanen, M. Zakrzewski, P. Moilanen, K. E. Lilja, S. Rajala, *Synth. Met.* **2012**, *162*, 1987.

[4] S. Tuukkanen, T. Julin, V. Rantanen, M. Zakrzewski, P. Moilanen, D. Lupo, *Jpn. J. Appl. Phys.* **2013**, *52*, 05DA06.

[5] S. Tuukkanen, M. Hoikkanen, M. Poikelispää, M. Honkanen, T. Vuorinen, M. Kakkonen, J. Vuorinen, D. Lupo, *Synth. Met.* **2014** (in press).

[6] S. Tuukkanen, S. Streiff, P. Chenevier, M. Pinault, H.-J. Jeong, S. Enouz-Vedrenne, C. S. Cojocaru, D. Pribat, J.-P. Bourgoin. *Appl. Phys. Lett.* **2009,** *95*, 113108.

[7] D.S. Hecht, R.B. Kaner, *MRS Bulletin* **2011**, *36*, 749.

[8] S. Lehtimäki, M. Li, J. Salomaa, J. Pörhönen, A. Kalanti, S. Tuukkanen, P. Heljo, K. Halonen, D. Lupo, *Int. J. Elect. Power Energy Syst.* **2014**, *58*, 42.

[9] S. Lehtimäki, J. Pörhönen, S. Tuukkanen, P. Moilanen, J. Virtanen, D. Lupo. *Mater. Res. Soc. Symp. Proc.* **2014**, *1659*.

[10] S. Lehtimäki, S. Tuukkanen, J. Pörhönen, P. Moilanen, J. Virtanen, M. Honkanen, D. Lupo, *Low-cost, Solution processable carbon nanotube nanocomposite supercapacitors and their characterization*, unpublished.

[11] M. Kaempgen, C. K. Chan, J. Ma, Y. Cui, G. Gruner, *Nano Lett.* **2009**, *9*(5), 1872

[12] C. Z. Meng, C. H. Liu, S. S. Fan, *Electrochem. Commun.* **2009**, *11*, 186.

[13] S. Kirchmeyer, K. Reuter, *J. Mater. Chem.* **2005**, *15*, 2077.

[14] A. Elschner, W. Lövenich. *MRS Bulletin* **2011**, *36*, 794.

[15] M. Frisch, J. Heydekorn, R. Dachselt, *ITS '09 Proceedings of the ACM International Conference on Interactive Tabletops and Surfaces* **2009**, 149.

[18] F. N. Eventoff, *U.S. Patent No.* 4313227, **1979**.

[19] I. Rosenberg, K. Perlin, *ACM Trans. Graph.* **2009**, *28*(3), 65.

[20] E. Choi, J. Kim, S. Chun, A. Kim, K. Lee, M. Jeong, C. Lim, T. Isoshima, M. Hara, S.-B. Lee, *J. Nanosci. Nanotechnol.* **2011**, *11*(7), 5845.

[21] *Touch technology brief, Projected capacitive technology,* 3M, **2013**.

[22] P. Dietz, L. Darren, *UIST '01 Proceedings of the 14th annual ACM symposium on User interface software and technology* **2001**, 219.

[23] S. P. Jobs, *U.S. Patent No.* 7479949B2, **2009**.

[24] W. Westerman, *Hand Tracking, Finger Identification and Chordic Manipulation on a Multi- Touch Surface,* PhD thesis, University of Delaware, **1999**.

[25] K. Kim, K. Shin, J.-H. Han, K.-R. Lee, W.-H. Kim, K.-B. Park, B.-K. Ju, J.J. Pak, *Electronics Lett.* **2011**, *47*(2), 118.

[26] NXP Semiconductors, AN11122, *Water and condensation safe touch sensing with the NXP capacitive touch sensors*, Application note, **2014**.

[27] T. Gary, *Projected Capacitive Touch Panels Designed for Marine Applications*, Ocular, **2013**.

[28] G. M. Krishna, K. Rajanna, *IEEE Sensors J.* **2004***, 4*(5), 691.

[29] M. Zirkl, G. Scheipl, B. Stadlober, A. Haase, L. Kuna, J. Magnien, G. Jakopic, J. R. Krenn, A Sawatdee, P. Bodö, P. Andersson, *Procedia Engineering* **2010**, *5*, 725.

[30] M. Zirkl, A Sawatdee, U. Helbig, M. Krause, G. Scheipl, E. Kraker, P. A. Ersman, D. Nilsson, D. Platt, P. Bodö, S. Bauer, G. Domann, B. Stadlober, *Adv. Mater.* **2011**, *23*, 2069.

[31] C. Rendl, P. Greindl, M. Haller, M. Zirkl, B. Stadlober, P. Hartmann, *UIST '12 Proceedings of the 25th annual ACM symposium on User interface software and technology* **2012**, *509*.

[32] S. Rajala, J. Lekkala. *IEEE Sensors J.* **2012**, *12*, 439.

[33] S. Kärki, J. Lekkala, H. Kuokkanen, J. Halttunen. *Sens. Actuators A Phys.* **2009,** *154*, 57.

[34] J. Pörhönen, S. Rajala, S. Lehtimäki, S. Tuukkanen, "Flexible Piezoelectric Energy Harvesting Circuit with Printable Supercapacitor and Diodes". *IEEE Trans. Electron Dev.* (accepted for publication).

[35] S. P. Beeby, M. J. Tudor, N. M. White. *Meas. Sci. Technol.* **2006**, *17*, R175.

[36] H. S. Kim, J.-H. Kim, J. Kim. *International Journal of Precision Engineering and Manufacturing* **2011**, *12*, 1129.

[37] J. G. Rocha, L. M. Gonçalves, P. F. Rocha, M. P. Silva, S. Lanceros-Méndez, *IEEE Trans. Ind. Electron.* **2010**, *57*(3), 813.

[38] A. Khaligh, P. Zeng, C. Zheng, *IEEE Trans. Ind. Electron.* **2010**, *57*(3), 850.

[39] S. C. Xu, B. Y. Man, S. Z. Jiang, C. S. Chen, C. Yang, M. Liu, X. G. Gao, Z. C. Sun and C. Zhang, *Appl. Phys. Lett.* **2013**, *102*, 151902.

[40] K. Y. Shin, J. Y. Hong, J. Jang, *Chem Commun.* **2011**,*47*(30), 8527.

[41] *Plastics – Determination of water absorption,* European standard ISO 62:2008.

[42] *Measurement Specialties Inc., Piezo film sensors, Technical manual.* Available online at: http://www.meas-spec.com (accessed 7 January 2014).

[43] A. Vinogradov, *Piezoelectricity in polymers*, Encyclopedia of Smart Materials, John Wiley & Sons, 2000.

[44] H. Topsoe, *Geometric correction factors in four point resistivity measurement, Bulletin* **1968**, *472-13* Available online at: http://www.fourpointprobes.com/haldor.html (accessed online 11 February 2014).